Performance of the GlueX Detector Systems

GlueX-doc-27xx

Gluex Collaboration

July 2015

Abstract

This document summarizes the status of calibration and performance of the GlueX detector as of summer 2015.

Introduction

1 Beamline and Tagger Elements

The Tagger Hodoscope

The Tagger Microscope

The Triplet Polarimeter

The Pair Spectrometer

2 The GlueX Detector

Start Counter

The quantities that measure the performance of the start counter are the timing resolution, σ_t, the efficiency of detecting a charged track, ϵ, and the maximum rate at which the detector can run. Performance values are listed in Table **??**. Figure 1 shows the timing resolution in element 29, where $300\,ps$ has been achieved. Carrying out this fit for each of the 30 start counter elements yields the plot shown in Figure 2.

Measure	Design	Current	Comment
σ_t	$350\,ps$	$\sim 300\,ps$	
ϵ	95 %		
Maximum rate			

Table 1: The performance of the start counter.

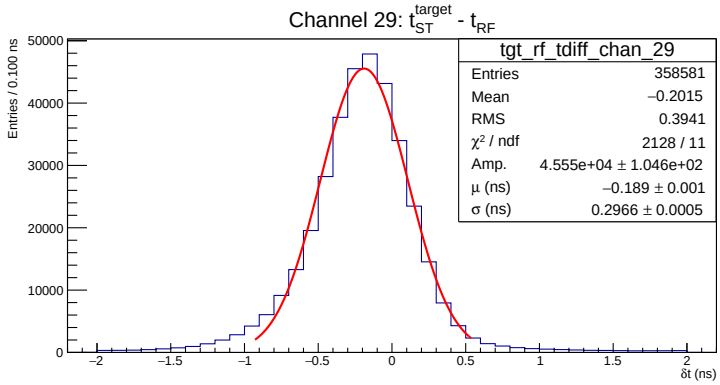

Figure 1: The time resolution of the start counter element 29 showing $300\,ps$ resolution.

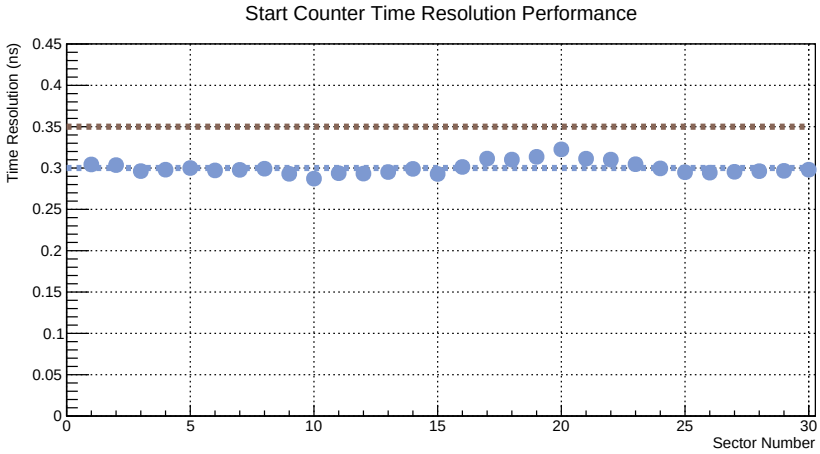

Figure 2: The time resolution of the start counter as a function of the start counter element number. The brown dashed line shows the design resolution, the blue points show the per element resolution.

Central Drift Chamber

The quantities to measure performance of the CDC are the resolution on the distance from the wire, $\sigma_{r\phi}$, and the per wire efficiency, ϵ_{wire}. Both of these are functions of the distance from the wire, and to some extent, the polar angle of the tracks. The resolution, $\sigma_{r\phi}$ becomes worse close to the wire because the isochrones (regions of constant electron arrival times) get smaller. This in turn makes it less probable to have a primary cluster produced on the shortest time isochrone. The efficiency, ϵ_{wire}, decreases close to the straw walls as due to the shorter track length in the active volume of the cell. The best measure of z resolution is the vertex resolution pairs of tracks detected in the CDC. Both z_{vert} and xy_{vert} are reported.

Measure	Design	Current	Comment
$\sigma_{r\phi}$	$150\,\mu m$	$\sim 200\,\mu m$	
ϵ_{wire}	95 %		
z_{vert}		$3\,mm$	From two tracks.
xy_{vert}			From two tracks.
Maximum rate			

Table 2: The performance of the central drift chamber.

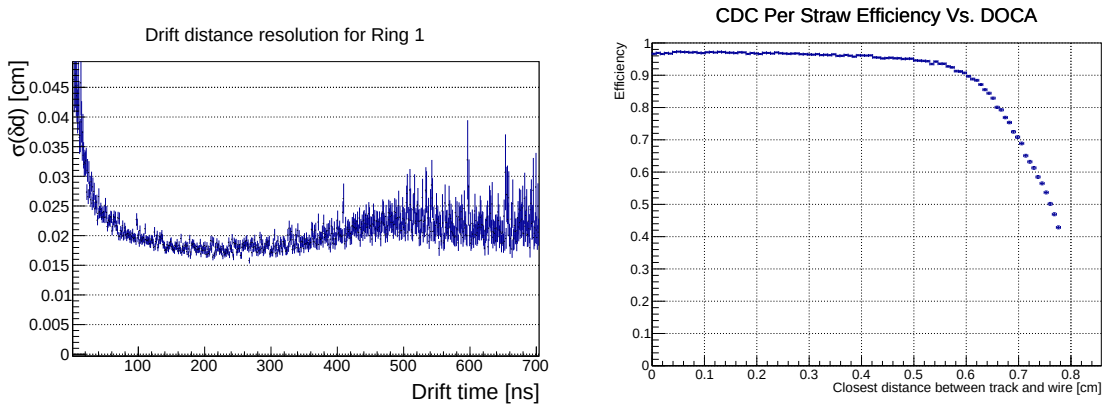

Figure 3: The position resolution, $\sigma_{r\phi}$ of the CDC as a function of drift time.

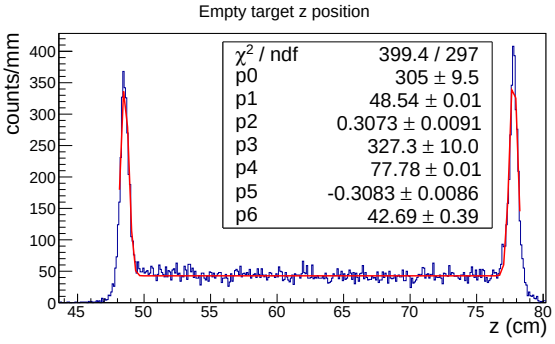

Figure 4: The z resolution at the target can be extracted from the empty target runs. The width of the thin target walls represent a measurement of z_{vert} of $3\,mm$.

Forward Drift Chamber

The performance parameters for the FDC were estimated using straight (no magnetic field) secondary tracks from the photon beam. In the FDC chambers we use the drift time to reconstruct the hit position in direction perpendicular to the wire (x), and the information from the strips of the two cathodes for the hit position along the wire (y).

The wire resolution as function of the distance to the wire is shown in Fig.5(left). The gas mixture used in the chamber, 40/60 Ar/CO_2, is characterized with a big slope of the the time-to-distance function at small distances, resulting in deterioration of the resolution in that region. Such gas mixture was chosen to minimize the magnetic field corrections. The resolution at big distances to the wire is affected by the non-uniformity of the electric field there.

The cathode strips register the avalanche produced very close to the wire, not the actual hit. Therefore, the cathode resolution (see Fig.5(right)) in x direction can be inferred simply from the reconstruction of the wire positions (blue points). On the other hand, the cathode resolution in y can be estimated by comparing the reconstructed avalanche position and the expected hit from the external tracking (red points). Note that due to the strip orientations w.r.t the wires, the x-resolution is expected to be about four times worse than the y-resolution. For the x-resolution, plotted as function of the charge, we see typical improvement of the resolution at higher charges. This is not the case for the y-resolution meaning there is a room for further improvement.

Every chamber is capable of reconstructing a 3D hit position using both, wire and cathode information. The efficiency for such reconstruction is demonstrated in Fig.6. It is $\sim 95\%$ except for that places with bad cathode channels ($< 1\%$).

Measure	Design	Current	Comment
σ_x	$200\,\mu m$	$170\,\mu m$	wire resolution for distances $1 - 4.5$ mm from wire
σ_y	$200\,\mu m$	$200\,\mu m$	cathode resolution from track residuals in y direction
ϵ_{3Dhit}		$\sim 95\,\%$	

Table 3: The performance of the Forward Drift Chamber. Parameters estimated with straight tracks without magnetic field.

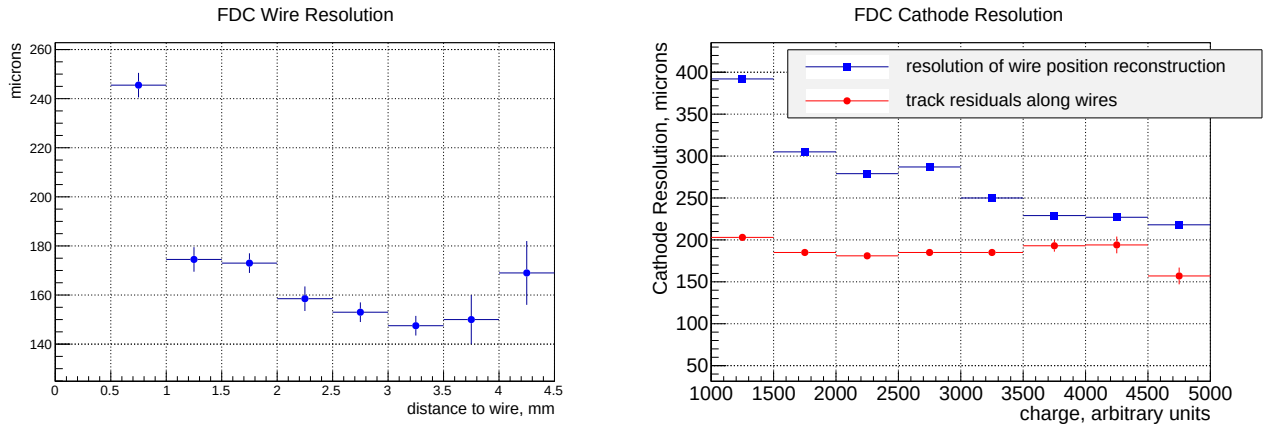

Figure 5: The FDC position resolutions: (left) from wires in x direction, σ_{wire}, as function of distance to the wire and (right) from cathodes, $\sigma_{cathode}$, in x (blue) and y (red) direction as function of the hit charge. Cathode x-resolution should be scaled down by factor of 3.86 to compare with y-resolution.

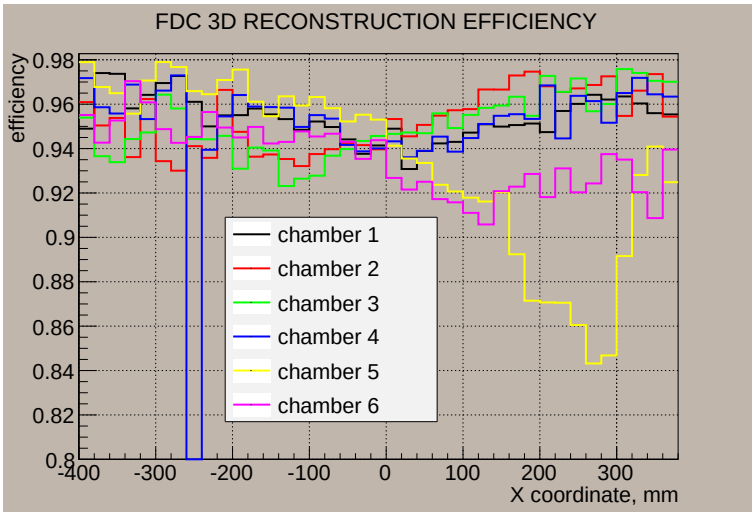

Figure 6: The combined (wire and cathode) 3D hit reconstruction efficiency for the six chambers of third FDC package vs wire position. The dips in the efficiencies correspond to bad cathode channels, most numerous in this package.

Barrel Calorimeter

Forward Calorimeter

Time-of-flight Wall

The time-of-flight wall is expected to have a per-paddle time resolution, σ_t, of $100\,ps$.

Measure	Design	Current	Comment
σ_t	$100\,ps$	$96\,ps$	
πp separation at $2\,GeV$		$9.55\,\sigma$	
πp separation at $3\,GeV$		$4.65\,\sigma$	
πK separation at $1\,GeV$		$9.35\,\sigma$	
πK separation at $1.5\,GeV$		$3.65\,\sigma$	

Table 4: The performance paramters of the time-of-flight system.

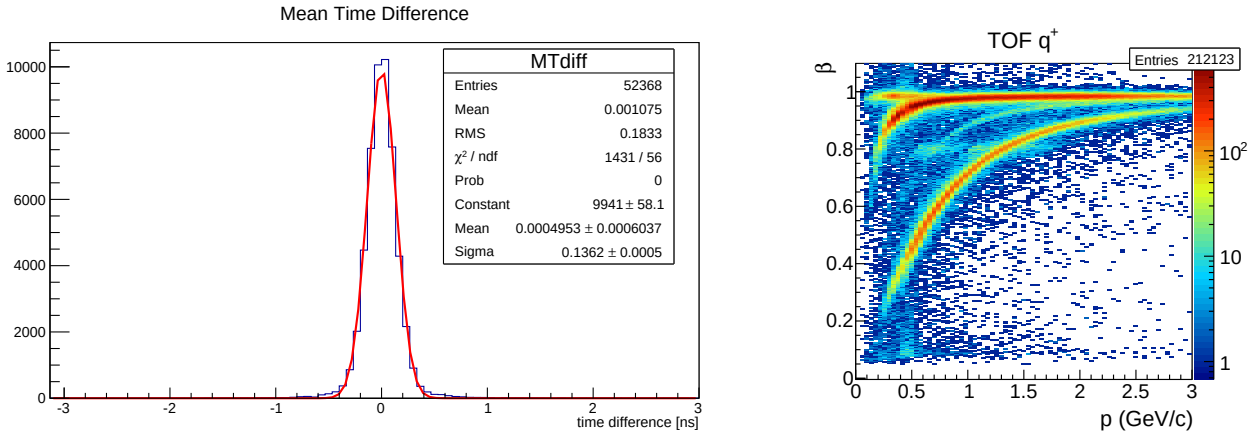

Figure 7: (left) The time difference between the summed time in the two layers of time-of-flight paddles. The $136\,ps$ sigma meaurement corresponds to $96\,ps$ time resolution per layer. (right) The β versus p plot for positive particles. Clear bands are seen for e^+, π^+, K^+ and p (top to bottom).

Data Aquisition and Trigger

Data Acqusition System

Level-1 Trigger

3 Summary